PNAS RESEARCH ARTICLE | MICROBIOLOGY OPEN ACCESS

Ferredoxin reduction by hydrogen with iron functions as an evolutionary precursor of flavin-based electron bifurcation

Max Brabender[a,1,2], Delfina P. Henriques Pereira[b,1], Natalia Mrnjavac[a,1], Manon Laura Schlikker[a], Zen-Ichiro Kimura[a,c], Jeerus Sucharitakul[d], Karl Kleinermanns[e], Harun Tüysüz[f], Wolfgang Buckel[g,h,i], Martina Preiner[b], and William F. Martin[a]

Edited by Caroline Harwood, University of Washington, Seattle, WA; received October 31, 2023; accepted February 14, 2024

Autotrophic theories for the origin of metabolism posit that the first cells satisfied their carbon needs from CO_2 and were chemolithoautotrophs that obtained their energy and electrons from H_2. The acetyl-CoA pathway of CO_2 fixation is central to that view because of its antiquity: Among known CO_2 fixing pathways it is the only one that is i) exergonic, ii) occurs in both bacteria and archaea, and iii) can be functionally replaced in full by single transition metal catalysts in vitro. In order to operate in cells at a pH close to 7, however, the acetyl-CoA pathway requires complex multi-enzyme systems capable of flavin-based electron bifurcation that reduce low potential ferredoxin—the physiological donor of electrons in the acetyl-CoA pathway—with electrons from H_2. How can the acetyl-CoA pathway be primordial if it requires flavin-based electron bifurcation? Here, we show that native iron (Fe^0), but not Ni^0, Co^0, Mo^0, NiFe, Ni_2Fe, Ni_3Fe, or Fe_3O_4, promotes the H_2-dependent reduction of aqueous *Clostridium pasteurianum* ferredoxin at pH 8.5 or higher within a few hours at 40 °C, providing the physiological function of flavin-based electron bifurcation, but without the help of enzymes or organic redox cofactors. H_2-dependent ferredoxin reduction by iron ties primordial ferredoxin reduction and early metabolic evolution to a chemical process in the Earth's crust promoted by solid-state iron, a metal that is still deposited in serpentinizing hydrothermal vents today.

acetyl CoA pathway | transition metals | serpentinization | origin of metabolism | origin of life

Significance

In the most ancient biochemical pathway known—the reductive acetyl-CoA pathway—the energy to fix CO_2 comes from geochemically produced H_2 gas, not from the sun. Cells that fix CO_2 with H_2 require an energetic trick: They split the electron pair in H_2, boosting the energy of one electron at the expense of the other to charge an ancient protein called ferredoxin with electrons. That requires enzymes and cofactors. How was ferredoxin charged before enzymes and cofactors arose? In alkaline, H_2-producing hydrothermal systems, the electron-donating potential of H_2 can reduce ferredoxins but requires the presence of a transition metal. We show that in water, raw iron will transfer electrons from H_2 to ferredoxin, uncovering a missing link in early metabolic evolution.

Autotrophic theories for life's origins posit that the first organisms on Earth were CO_2-fixing microbes. In that view, relicts from primordial CO_2 fixation might have been preserved in modern metabolism, bringing CO_2 fixation pathways to bear the origin of metabolism and life (1). Among known routes of CO_2 fixation, the acetyl-CoA pathway is the most ancient (2). It is the only CO_2 fixation pathway known to operate in both archaea (methanogens) and bacteria (acetogens) (3) and the only one that is exergonic, releasing energy in the synthesis of acetyl-CoA ($CH_3COSCoA$) from H_2, CO_2, and coenzyme A (CoASH) via formate as an intermediate (4) according to

$$2CO_2 + 4H_2 + CoASH \rightarrow CH_3COSCoA + 3H_2O,$$

with $\Delta G_o' = -59$ kJ/mol (2). Roughly 70% of the resulting acetyl-CoA pool is further converted to pyruvate (CH_3COCOO^-) by ferredoxin-dependent CO_2 fixation at the pyruvate synthase reaction

$$2Fd_{red} + CO_2 + H^+ + CH_3COSCoA \rightarrow 2Fd_{ox} + CoASH + CH_3COCOO^-,$$

for the synthesis of amino acids, bases, cofactors, and cell mass (2). The enzymes of the acetyl-CoA pathway are replete with transition metals as electron carriers and catalysts (4–8), inorganic cofactors that are reasonably interpreted as relicts (9–12) from a geochemical setting (13) within which metabolism and life arose. In acetogens and methanogens growing on H_2 and CO_2, the acetyl-CoA pathway converts H_2 and CO_2 into formate (4), acetate, and pyruvate (2) via ~10 enzymatic reactions that require 14 cofactors and 127 proteins, including the cofactor biosynthesis pathways (14).

Newer findings reveal that under the conditions of H_2-producing (serpentinizing) hydrothermal vents (15, 16), the function of those 127 proteins can be replaced in toto by individual transition metal minerals such as Ni_3Fe or Fe_3O_4 in vitro. These catalysts not only convert CO_2 and H_2 with high specificity to formate, acetate, and pyruvate in the laboratory (17–20), they are deposited in serpentinizing hydrothermal vents in nature (21–23). They can even convert H_2 and CO_2 to pyruvate at concentrations of 200 μM (19), the physiological pyruvate concentration in the cytosol of acetogens growing on H_2 and CO_2 (24). Whether catalyzed by enzymes or metals, these ancient metabolic reactions

Author contributions: M.B., D.P.H.P., N.M., M.P., and W.F.M. designed research; M.B., D.P.H.P., and M.L.S. performed research; J.S. and H.T. contributed new reagents/analytic tools; M.B., D.P.H.P., N.M., Z.-I.K., K.K., W.B., M.P., and W.F.M. analyzed data; M.B., D.P.H.P., N.M., M.L.S., Z.-I.K., J.S., K.K., H.T., W.B., M.P., and W.F.M. edited the paper; and M.B., D.P.H.P., N.M., and W.F.M. wrote the paper.

The authors declare no competing interest.

This article is a PNAS Direct Submission.

[1]M.B., D.P.H.P., and N.M. contributed equally to this work.

[2]To whom correspondence may be addressed. Email: max.brabender@hhu.de.

This article contains supporting information online at https://www.pnas.org/lookup/suppl/doi:10.1073/pnas.2318969121/-/DCSupplemental.

Published March 21, 2024.

go forward because in the reaction of H_2 with CO_2, the equilibrium lies on the side of reduced carbon compounds (25). Transition metal catalysts forge a functional link between ancient metabolism and modern serpentinizing hydrothermal systems, which synthesize formate via abiotic geochemical reactions in amounts sufficient to support microbial growth (26–30).

Though the reactions of the acetyl-CoA pathway naturally unfold from H_2 and CO_2 in the presence of transition metal catalysts in the laboratory, this does not, by itself, solve the problem of metabolic origins, because the biochemically catalyzed acetyl-CoA pathway as it occurs in cells presents a thermodynamic paradox. The CO_2-reducing enzymes of the acetyl-CoA pathway require reduced ferredoxin, Fd, as their electron donor, whereby Fd is reduced with electrons from H_2 via hydrogenases (Fig. 1). However, the midpoint potential of H_2 under standard physiological conditions, $E_o' = -414$ mV, is more positive than the midpoint potential of low potential ferredoxins, roughly –450 to –500 mV in cells (31) as required for CO_2 fixation ($E_o' = -430$ mV), making Fd reduction with H_2 a steeply endergonic process (Fig. 1*A*), especially in environments with low H_2 partial pressures (31). How do cells push electrons energetically uphill to Fd for CO_2 fixation?

The discovery of flavin-based electron bifurcation (32, 33) revealed how the main groups of H_2-dependent autotrophs, methanogens and acetogens, reduce ferredoxin with H_2 (34, 35). The two electrons from H_2 are transferred via a hydrogenase (36, 37) to an enzyme-bound flavin, where they diverge along exergonic and endergonic paths, respectively. One electron is transferred to a high potential acceptor such as NAD^+ or the heterodisulfide CoM-S-S-CoB, the other is transferred, in strict stoichiometry, to Fd as the low potential acceptor (Fig. 1*A*). Reduction of the high potential acceptor renders the overall Fd-reducing reaction exergonic (31–42). All flavin-based electron bifurcation redox couples known so far reduce Fd (39) or flavodoxins under Fe limitation (41). This indicates that the ancestral physiological function of flavin-based electron bifurcation was to supply reduced Fd as a low potential reductant for metabolism, in turn welding both flavin-based electron bifurcation and Fd into the foundation of autotrophic theories for the origin of metabolism because, in concert, they supply the electrons for FeS and FeNiS clusters in enzymes of the acetyl-CoA pathway (2–8, 31, 35, 43, 44).

While flavin-based electron bifurcation solves the bioenergetic problem of Fd reduction with H_2 in metabolism, it presents a paradox in prebiotic physiology (45, 46): Given the antiquity of the acetyl-CoA pathway, how was Fd reduced in early evolution i) before the origin of the more complicated Fe–Ni and Fe–Fe hydrogenases that oxidize H_2 (Fig. 1*B*) and ii) before the origin of the vastly more complicated multi-enzyme process of flavin-based electron bifurcation (31–42) (Fig. 1*A*) that is required for Fd reduction in H_2-dependent chemolithoautotrophs? Because of its universality among anaerobes, and by functional, structural, and biogenetic simplicity (Fig. 1*B*), Fd is clearly more ancient than the hydrogenases (Fig. 1*C*) that supply reduced ferredoxin as the reductant for CO_2 fixation. The FeS clusters of Fd are not only simpler in structure than hydrogenase active sites, which extract electrons from H_2 for Fd reduction, they also lack the small molecule ligands that are added to iron during hydrogenase active site maturation (47–49) (Fig. 1*C*) by maturases that arose subsequent to the hydrogenase structural protein (50). In early biochemical evolution, simpler mechanisms must have therefore preceded hydrogenases and flavin-based electron bifurcation as a means of supplying reduced ferredoxin, though such mechanisms have not been experimentally identified so far. Here, we investigate the ability of native transition metals to reduce ferredoxin with H_2 in the absence of flavins or electron-bifurcating enzymes.

Results

We used H_2 as the source of electrons for Fd reduction because it is the reductant that drove primary production on Earth prior to the origin of photosynthesis starting with the first signs of life 3.8 billion years ago (51, 52). To activate H_2 we used native metals and metal alloys that are naturally deposited in serpentinizing systems (21–23). Serpentinization entails geochemical redox reactions between Fe(II) minerals and H_2O circulating through the Earth's crust (15, 16), generating H_2 as the source of energy and electrons for primary production by bifurcation-dependent anaerobic autotrophs that inhabit serpentinizing systems in the dark subsurface: acetogens (26, 53) and methanogens (27, 28). For assays, we used glass vials and 5 bar of H_2, corresponding to 3.8 mM H_2 in the aqueous phase, well within the range of H_2 concentrations measured in the effluent of Lost City (29, 54) and other serpentinizing hydrothermal systems (46, 55). The reduction of ferredoxin from *Clostridium pasteurianum* purified from *Escherichia coli* can be followed by the standard photometric assay (56) by following the difference in absorption at 420 nm (Fig. 2).

Previous studies showed that Fe^0, Ni^0, and Co^0 can catalyze the reduction of NAD^+ to NADH under mild hydrothermal conditions: 5 bar H_2, 40 °C (57). NAD^+ is a stronger oxidant ($E_o' = -320$ mV) than *C. pasteurianum* Fd ($E_o' = -412$ mV) (58) and NAD^+ reduction is a two-electron reaction involving hydride (H^-) transfer while ferredoxin reduction involves one-electron transfer to [4Fe4S] centers. A screen of transition metals revealed that Ni^0, Co^0, Mo^0, NiFe, Ni_2Fe, Ni_3Fe, and Fe_3O_4 do not mediate H_2-dependent Fd reduction, whereas Fe^0 reduces Fd in the presence of H_2 (Fig. 3). The concentration of Fd in reactions was 30 μM, slightly lower than the physiological concentration in anaerobes, where Fd concentrations are in the range of 80 to 400 μM (59).

Ferredoxin reduction by Fe^0 required roughly four hours at 40 °C (Fig. 4). Notably, *C. pasteurianum* Fd does not autoreduce under these conditions, as shown in Fig. 4 for reactions of Fd and H_2 without metal. This is also seen in reactions of Fig. 3 where no Fd reduction was detected. Ferredoxin reduction with Fe^0 at pH 8.5 required H_2 and solid-state iron (Fig. 3). The lack of autoreduction is noteworthy, because FeNiS and FeS enzymes of the acetyl-CoA pathway (acetyl-CoA synthase/carbon monoxide dehydrogenase and pyruvate synthase) are able to activate H_2 via latent hydrogenase activities (60). However, *C. pasteurianum* Fd does not oxidize H_2, in agreement with the absence of hydrogenase activity for Fd from *Clostridium thermoaceticum* (60). The FeS clusters of *C. pasteurianum* Fd require an iron surface for reduction under the conditions tested here.

Early studies detected an effect of pH on the reduction of FeS proteins from *C. pasteurianum* and other sources, though the effects were generally small in the pH range of 6 to 9 (63). Subsequent studies did not detect pH-dependent effects (58). The conditions in our investigation are aligned with serpentinizing systems, where the midpoint potential of H_2 oxidation is directly influenced by pH through the reaction

$$H_2 \rightarrow 2e^- + 2H^+,$$

which is pulled to the right at alkaline pH via proton removal, resulting in very negative midpoint potentials. In actively serpentinizing hydrothermal systems, pH can exceed 10 and the midpoint potentials can exceed –700 mV (26, 30, 46, 55). We observed a tendency for the pH to increase with reaction time in runs with Fe^0 despite the presence of 133 mM P_i buffer. To see whether the observed Fd reduction is due solely to a pH

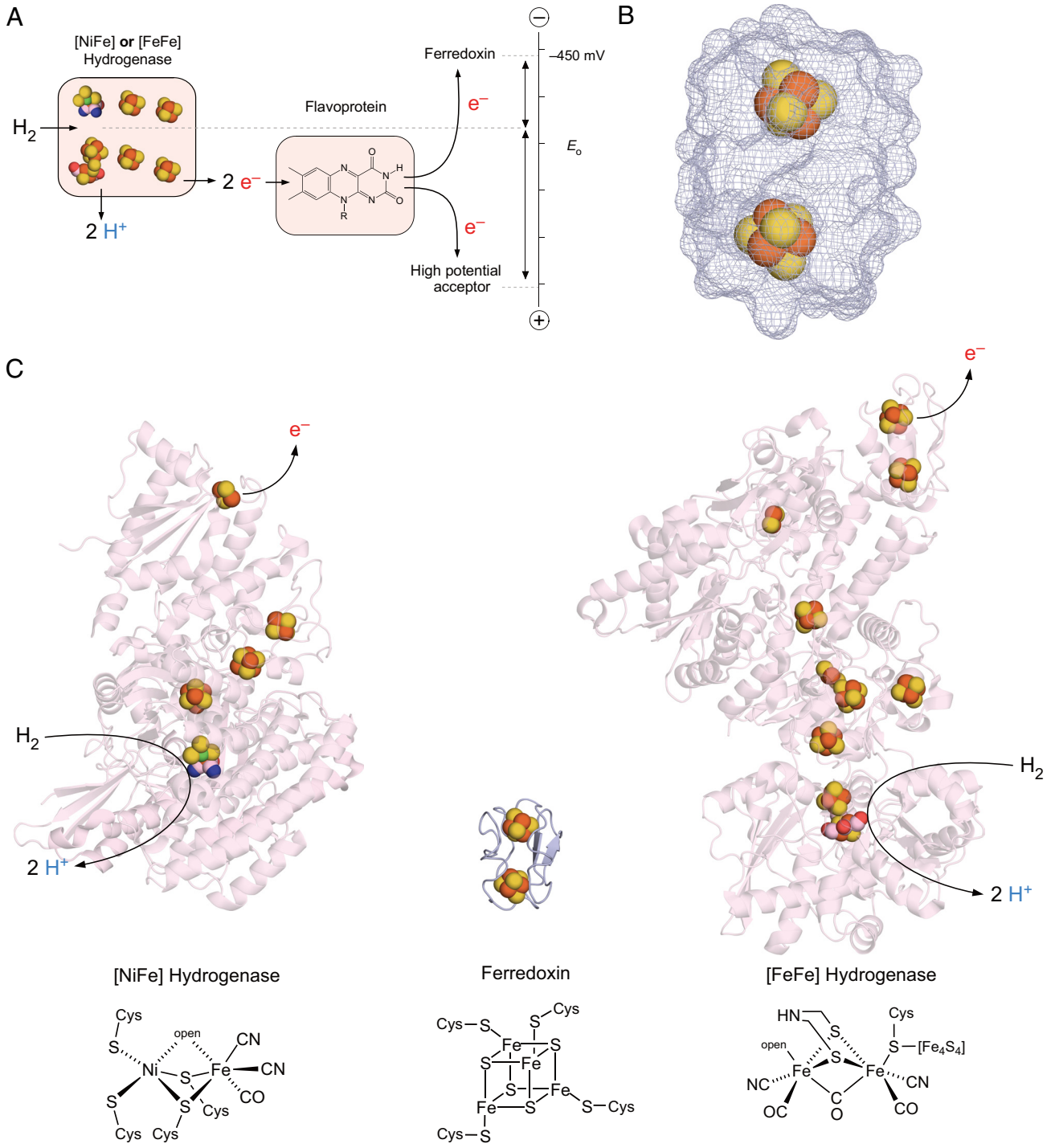

Fig. 1. Ferredoxin is the primordial one-electron carrier in metabolism. (*A*) Flavin-based electron bifurcation is required to reduce low potential ferredoxin for CO_2 fixation using electrons from H_2 (schematic). The flavoprotein and its high potential acceptor varies across organisms and pathways (31–42). (*B*) The structure of *C. pasteurianum* ferredoxin (PDB ID: 1CLF). Other renderings of ferredoxin are given in *SI Appendix*, Fig. S1. (*C*) The structure of the two forms of hydrogenase used to oxidize H_2 for Fd reduction and their catalytic metal clusters compared to Fd from *C. pasteurianum*. The structures are for MvhAGD, the [NiFe] hydrogenase from *Methanothermococcus thermolithotrophicus* (PDB ID: 5ODC) (36) and HydABC, the [FeFe] hydrogenase from *Acetobacterium woodii* (PDB ID: 8A5E) (37). The CN^- and aminodithiolate ligands are missing in the structure of the H-cluster of HydABC. One protomer of HydABC and one protomer of MvhAGD are shown, the biologically active complexes being a homodimer of heterotrimers and a homodimer of heterohexamers (including the heterodisulfide reductase), respectively. Under nickel limitation, some methanogens express a third form of hydrogenase with a unique iron-guanylylpyrinidol cofactor that transfers electrons from H_2 directly to methenyl-tetrahydromethanopterin without FeS cluster intermediates (8).

effect (altered midpoint potential of H_2 oxidation) on metal-dependent water reduction, native metals were tested at pH 10. For Ni^0 and Co^0, there was no observable Fd reduction with H_2 at pH 8.5 or pH 10 (Fig. 5*B*). At pH 8.5, Fd reduction required Fe^0 and H_2, while at pH 10, there was also substantial Fd reduction without addition of exogenous H_2 (Fig. 5*A*). This was expected based on findings from NAD^+ reduction using ^2H labeling, where it was observed that at pH 10, Fe^0 generates endogenous $^2H^-$ from

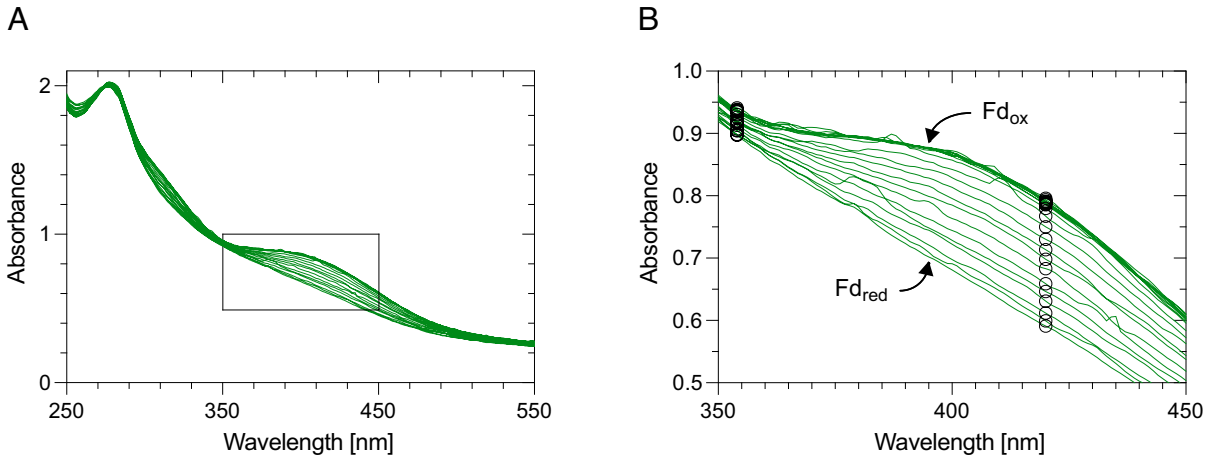

Fig. 2. Photometric assay of Fd reduction. (*A*) UV-Vis spectra following the oxidation of 30 μM of reduced Fd from *C. pasteurianum* in 0.133 M phosphate buffer at pH 8.5 through air exposure for 300 s. Fd was previously reduced through addition of two equivalents of sodium dithionite ($Na_2S_2O_4$). (*B*) Magnified boxed region in A showing the difference in absorption of the [4Fe4S] clusters at 420 nm and the isosbestic point at 354 nm (56), used for normalization. The time course of Fd reduction is shown in *SI Appendix*, Fig. S2.

^2H_2O (57). The yield of reduced ferredoxin for Fe^0 without H_2 at pH 10 relative to the yield without H_2 at pH 8.5 (Fig. 5*A*) might result from the more negative H_2 midpoint potential at increased pH. Reduction of Fd cannot be tested with ^2H_2O in the same way as for NAD^+ (57) because Fd accepts single electrons rather than hydride. Surface oxidation of Fe^0 can generate soluble Fe^{2+} (64–66), which is not, however, a sufficiently strong reductant to reduce ferredoxin ($Fe^{2+} \rightarrow Fe^{3+} + e^-$, $E_o' = -200$ mV) (67).

To further probe the effect of pH, we increased the buffer strength to 1.33 M P_i and incubated in the presence of H_2 at different pH values (Fig. 6). At pH 7, where the midpoint potential of the H_2 oxidation is $E_o = -414$ mV, close to the midpoint potential of Fd, the reaction is incomplete. At pH 6, the reaction is blocked, as expected. Ferredoxin reduced by H_2 over Fe^0 is biologically active, it serves as a substrate to reduce $NADP^+$ in the reaction catalyzed by ferredoxin:NADP oxidoreductase from spinach chloroplasts (*SI Appendix*, Fig. S4).

Discussion

In water at 40 °C, H_2 can reduce *C. pasteurianum* Fd at a concentration of 30 μM in the presence of Fe^0 within a few hours. The pH and partial pressure of H_2 used (5 bar, roughly 3.8 mM in solution according to Henry's law) correspond to conditions in actively serpentinizing hydrothermal vents (29, 46, 54, 55). The 30 μM Fd concentration used is close to that in cells. We found that iron was effective in reducing Fd with H_2. Neither the Fe–Ni alloys tested nor magnetite were effective in Fd reduction. Though the mechanism of electron transfer from the heterogeneous Fe^0 surface to Fd is obscure, it requires Fe in the solid state in these experiments and likely entails chemisorption for H_2 activation (61, 62) with electron transfer mechanisms possibly similar to those that operate between FeS clusters in proteins (68, 69). Because Fe^0 conducts, H_2 oxidation and Fd reduction need not occur at the same site on iron particles. Several studies have used electrodes with externally applied potentials to promote

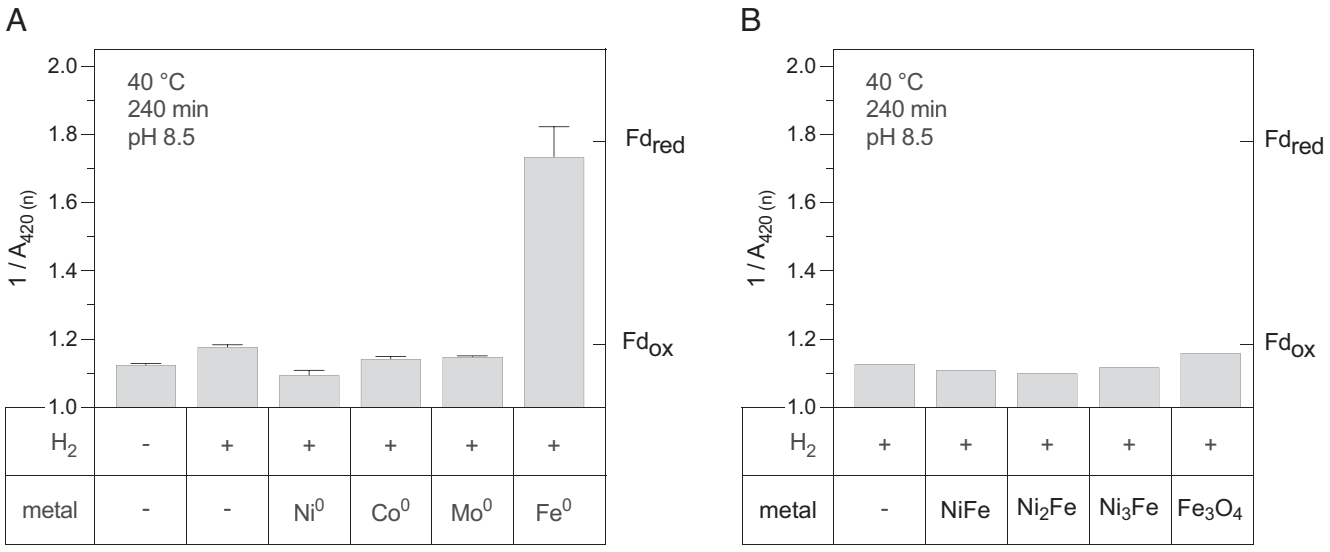

Fig. 3. Metals tested for H_2-dependent Fd reduction. Reaction of 30 μM Fd from *C. pasteurianum* with 0.1 mmol (*A*) native metal and (*B*) metal alloys and magnetite under a hydrogen atmosphere [5 bar] in 0.133 M phosphate buffer at pH 8.5. Normalized absorption of [4Fe4S] clusters in Fd is shown (*Methods*). Raw data for iron shown in *SI Appendix*, Fig. S3.

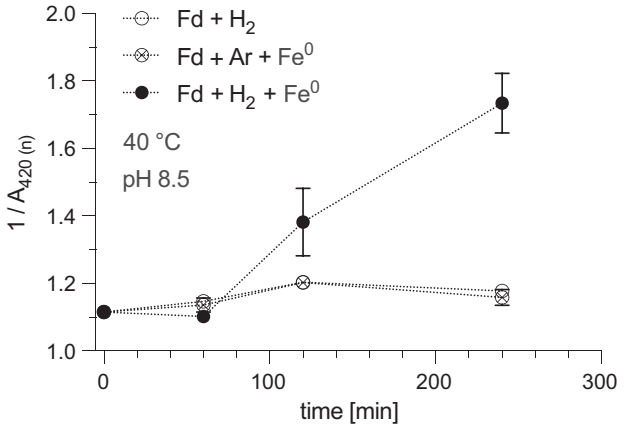

Fig. 4. Time course of Fe^0-promoted H_2-dependent Fd reduction. The lag time of about 1 h might reflect delayed formation of chemisorbed hydrogen on the iron surface (61, 62) or H_2-dependent formation of active sites on the metal surface. A similar lag time was observed for H_2-dependent NAD^+ reduction on Fe^0 (57).

prebiotic chemical reactions (70, 71). We applied no external potentials. At alkaline pH, serpentinization and Fe^0 produce the diffusible reductant H_2 by interactions with water. The reduction of Fd took place via redox reactions with exogenous H_2 and Fe^0 at pH 8.5 and without exogenous H_2 at pH 10. At pH 6, Fd reduction does not take place (Fig. 6). The reason why Fe^0 reduces Fd in our reactions while the other metals tested do not (Fig. 3) is likely due to the more negative midpoint potential of Fe^0 in reaction to the divalent ion relative to the other metals tested (57, 67) or to differences in H_2 chemisorption among metals tested (57), or both.

An Ancient Root to Modern Corrosion? Though motivated by the study of early evolution, our findings bear upon a modern problem: the corrosion of iron by microbes that use Fe^0 as an electron source. A number of H_2-dependent anaerobic microbes that use the acetyl-CoA pathway, most notably methanogens and acetogens, can use Fe^0 as an electron source for growth (64–66). Iron oxidation results in iron dissolution as Fe^{2+} and corrosion. The molecular mechanisms by which acetogens and methanogens extract electrons from Fe^0 are still unknown (66), but the transient formation of H_2 from oxide-generating reactions of iron and water—as suggested in a previous study of NAD^+ reduction (57) and as we suspect for Fd reduction without H_2 at pH 10 (Fig. 6)—are widely discussed (64–66).

While it is possible that use of Fe^0 as a source of electrons is a recent microbial adaptation to human metalworking technology, it is far more likely that this physiological capacity is ancient, a holdover from growth on ubiquitous Fe^0 and iron alloys (21–23) in serpentinizing systems, which are as old as water on Earth (15, 16). This would be highly compatible with phylogenetic and physiological evidence for the age of acetogens and methanogens (26, 53, 72–74), lineages that can grow on iron. Native metals are deposited in hydrothermal systems when serpentinization and H_2 production are active. When H_2 production through serpentinization stops, deposited Fe^0 is still available (21–23), which can serve as the sole electron source for several lineages of acetogens and methanogens (64–66). Our findings raise the possibility that FeS clusters localized in proteins at the cell surface mediate growth on iron as an electron source in organisms that do not use extracellular multiheme cytochromes (66) or extracellular flavins to access electrons.

No Requirement for Membranes or Ion Gradients. The enzymatic process of flavin-based electron bifurcation requires neither membranes, ion gradients, nor membrane-integral proteins (31–42), hence it could have operated at a very early stage of biochemical evolution, before the origin of free-living cells and even before the origin of membranes. During the course of evolution, microbes evolved membrane-dependent protein complexes that generate reduced ferredoxin without flavin-based electron bifurcation. These include the energy-conserving hydrogenase Ech, which taps ion gradients at the plasma membrane to reduce Fd with H_2 (75, 76). It has been proposed that Ech-like functions might have been required for primordial ferredoxin reduction (77, 78), yet Ech is

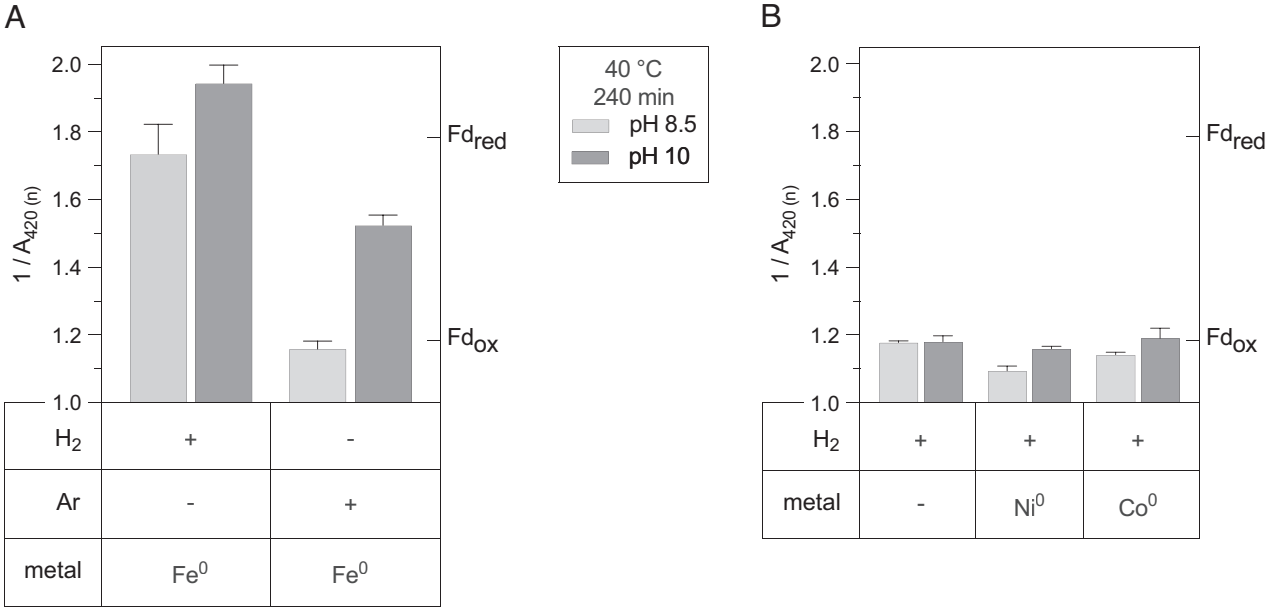

Fig. 5. H_2-dependent Fd reduction at pH 10. Reaction of 30 μM Fd from *C. pasteurianum* with 0.1 mmol metal. (*A*) Native iron and (*B*) native cobalt and native nickel under a hydrogen atmosphere [5 bar] in 0.133 M phosphate buffer at pH 8.5 and pH 10. Normalized absorption of [4Fe4S] clusters in Fd is shown (*Methods*).

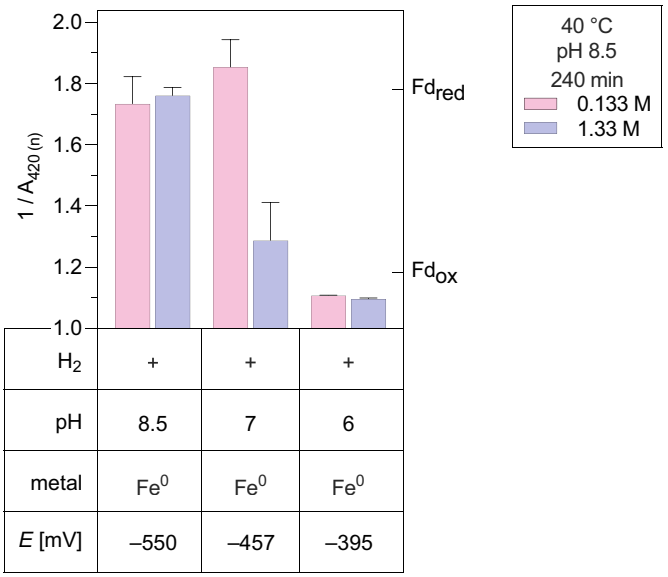

H_2	+	+	+
pH	8.5	7	6
metal	Fe^0	Fe^0	Fe^0
E [mV]	–550	–457	–395

Fig. 6. pH dependence of Fd reduction with H_2. Reaction of 30 μM Fd from *C. pasteurianum* with 0.1 mmol native iron under a hydrogen atmosphere [5 bar] in 0.133 M and 1.33 M phosphate buffer at pH 8.5. Normalized absorption of [4Fe4S] clusters in Fd is shown (*Methods*). The midpoint potential of H_2 was calculated using the Nernst equation.

evolutionarily derived from soluble Fe–Ni hydrogenases (79), which require electron bifurcation for autotrophic function, such that Ech can hardly be an ancestral Fd-reducing agent. Our findings show that neither ion gradients, membranes, nor Ech-like functions are required by the far simpler process of Fd reduction in the presence of H_2 and iron.

A Metal:Protein Hybrid Intermediate. In contrast to previous studies of inorganic-catalyzed prebiotic reactions (80), the substrate of our iron-dependent reaction is a protein with FeS clusters. Ferredoxin reduction with H_2 and Fe^0 under serpentinizing conditions closes an important gap in early bioenergetic evolution, providing an example of a hybrid intermediate state in the evolution of metabolism subsequent to abiotic versions of the acetyl-CoA pathway (17–20, 81) yet prior to the origin of enzymes that perform flavin-based electron bifurcation (Fig. 7). The ancestral route of pyruvate synthesis from H_2 and CO_2 is readily catalyzed by a number of different transition metal catalysts, including Fe^0, Ni^0, Ni_3Fe, and Fe_3O_4 (17–20) that occur naturally in serpentinizing hydrothermal vents (Fig. 7*A*). With the advent of genes and proteins, primitive versions of the acetyl-CoA pathway (72, 82) comprising the Fd-dependent enzymes carbon monoxide dehydrogenase/acetyl-CoA synthase and pyruvate synthase (5–8) could replace inorganically catalyzed pyruvate synthesis, but the activity of the soluble enzymes remained tied to transition metals in the crust for the supply of reduced ferredoxin as a kind of electrochemical umbilical cord connecting H_2 activation (solid phase) to one-electron supply at enzymes (aqueous phase) (Fig. 7*B*).

Given geochemical availability of H_2 from serpentinization and CO_2 from seawater, this hybrid intermediate state would be indefinitely sustainable, but metabolic evolution would remain bound to the Earth's crust by the requirement for solid-state metals. Escape from the crust required a number of inventions, among them cellularization and the ability to fix CO_2 without the requirement for physical contact between cytosolic enzymes and metals in the crust. The origin of hydrogenases (36, 37, 50) and flavin-based electron bifurcation freed H_2-dependent ferredoxin reduction from solid-state contact, but coupled Fd reduction to the simultaneous reduction of stronger oxidants (Fig. 7*C*). These eventually included NAD^+ via the electron-bifurcating Fe–Fe hydrogenase reaction of acetogens (35) or CoM-S-S-CoB via the MvhADG/HdrABC complex (Fe–Ni hydrogenase/heterodisulfide reductase) of methanogens (34), coupling Fd-dependent CO_2 reduction to stoichiometrically balanced energy metabolism in these H_2-dependent chemolithoautotrophs (39). The evolutionary innovation of flavin-based electron bifurcation enabled the use of H_2 as an electron donor for Fd reduction at cytosolic pH values near 7. Despite their divergent mechanisms of pumping for ATP synthesis (43, 44), the acetyl-CoA pathway links methanogens and acetogens (84), primordial members of the archaeal and bacterial lineages (72–74), with serpentinizing environments (15, 16, 85), which they still inhabit today (26–30, 53, 74). Our findings provide a crucial missing link in early metabolic evolution, closing a gap in autotrophic theories by demonstrating a functional intermediate state in the transition from geochemical to enzymatic catalysis in H_2-dependent CO_2 fixation (Fig. 7), as required if life

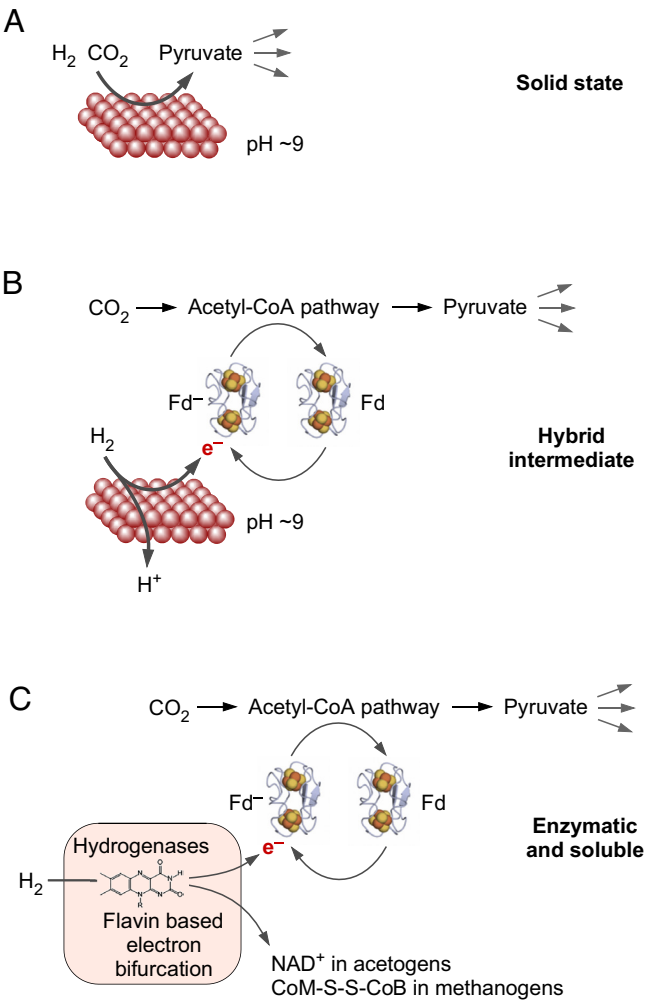

Fig. 7. Three phases in the evolution of autotrophy via the acetyl-CoA pathway. (*A*) Metal-catalyzed pyruvate synthesis from H_2 and CO_2 (17–20, 80) as the ancestral state of the acetyl-CoA pathway. (*B*) Iron-dependent ferredoxin reduction with H_2 as a source of the physiological reductant (reduced ferredoxin) for CODH/ACS (5, 7, 60) and PFOR (6, 34, 60) in an intermediate stage of physiological evolution before the origin of flavin-based electron bifurcation. (*C*) H_2 oxidation via Fe–Fe and Ni–Fe hydrogenases and flavin-based electron bifurcation for the synthesis of reduced ferredoxin in a fully soluble enzymatic system encoded by genes. The source of methyl groups for the ACS reaction in (*B*) can either be geochemical (72, 83) as in (*A*) or biochemical from CO_2 as in the extant acetyl-CoA pathway (2).

arose at hydrothermal vents (13) involving the acetyl-CoA pathway (83).

In the Light of Origin Theories. Do the present findings discriminate among theories for the origin of life? The main competing theories for origins encompass genetics first and metabolism first proposals. Genetics first theories posit, in current mainstream formulations, that RNA-based replicating systems preceded the origin of life-like metabolic pathways and that the RNA bases were synthesized with the help of atmospheric reactions giving rise to cyanide, $C{\equiv}N^-$, or C≡N-containing compounds that fueled RNA synthesis until metabolism arose (86–88). In genetics first theories, reactions between H_2 and CO_2 play no role, as the reduced carbon species that initiate primordial amino acid and nucleobase synthesis contain reduced carbon with highly reactive C≡N bonds (89–91). Because C≡N-containing compounds are absent in modern biosynthesis, genetics first models do not intersect microbial metabolism, such that flavin-based electron bifurcation, H_2-dependent CO_2 fixation, and the acetyl-CoA pathway do not address genetics first, and vice versa.

Metabolism first theories posit that organized and catalyzed chemical reaction networks having evident similarity to modern metabolic pathways are the starting point of life chemistry, from which genetic systems later emerged (92). In autotrophic theories, metabolism started from CO_2, just like it does in the primary production of modern ecosystems (1). Autotrophic theories that draw upon hydrothermal vents (13) and H_2 from serpentinization to reduce CO_2 via the acetyl-CoA pathway to pyruvate strictly require evolutionary precursors of electron bifurcation (45, 46), readily accommodating the present findings. From pyruvate, the central intermediate of biosynthesis (2, 93), the paths to the incomplete reductive reductive citric acid cycle (94), amino acids, nucleotide, and cofactor synthesis are short, entailing only about 400 reactions (95). Amino acid and nucleobase syntheses from biochemical starting compounds can take place without enzymes (80, 96, 97), as suggested in these pages in 1963: "primitive organic cofactors (along with inorganic ions) acting on surfaces were the original 'bio' catalysts, active long before specific polypeptides evolved" (92). As Fe^0 presents a surface, our findings (Fig. 7) are in full accord with that depiction.

Origins theories that start with methane oxidation (98, 99) belong to the metabolism first category but not to autotrophic theories, because they start from CH_4 as the first carbon source (methanotrophy) as opposed to CO_2 (autotrophy). Methane requires strong oxidants such as nitrogen oxides, O_2, or H_2O_2 to enter primordial metabolism (99), precluding a requirement for H_2 (98) hence electron bifurcation. Wächtershäuser explicitly excluded H_2 as the primordial source of electrons for metabolism, because of the uphill nature of CO_2 reduction with H_2 (100) under standard conditions. Smith and Morowitz (101) concluded that the site of life's origin must have performed electron bifurcation; our findings identify a simpler and functional environmental precursor. Other proposals involve electrogenesis, using externally applied voltages on transition metal electrodes to generate potentials required to reduce CO_2 without H_2 (71). These theories miss the impact of pH on H_2 oxidation.

Conclusion

Iron-mediated, H_2-dependent Fd reduction provides the function of electron bifurcation in water at H_2 partial pressures, temperatures, and pH that occur naturally at serpentinizing hydrothermal vents. It requires solid-state transition metal surfaces, with no need for sulfide minerals, membranes, ion gradients, redox cofactors, externally applied voltage, or oxidants other than Fd, presenting a simple (one gas, one solid) and energetically smooth transition in physiological evolution from abiotic to enzymatic use of H_2 from serpentinization to reduce Fd (Fig. 7). These findings point to an early phase of biochemical evolution in which proteins (ferredoxin), hence ribosomes and the code existed in the last universal common ancestor (72), but metabolic electron acquisition from H_2 during autotrophic origins was still tied to transition metals in serpentinizing systems in the Earth's crust. Acetogens, methanogens, other organisms that inhabit modern serpentinizing systems (26–30, 53, 74), and chemolithoautotrophs that fuel their acetyl-CoA pathway with electrons from H_2, native iron (64–66) or phosphite (102) might harbor additional biochemical relicts from the earliest phases of physiological evolution.

Methods

Reactions were prepared under anaerobic conditions in a glovebox (GS 79821, GS Glovebox-System), using N_2-washed 0.133 M or 1.33 M phosphate buffer in HPLC-grade water (pH 6, 7, 8.5 or 10; potassium phosphate monobasic and sodium phosphate dibasic (Honeywell Fluka)) containing Fd, pipetted into 5 mL glass vials (beaded rim) with metal powders (no powder in controls) and a polytetrafluoroethylene (PTFE)-coated stirring bar. Vials were sealed by a crimp cap with PTFE-coated membrane. To allow gas exchange, a syringe needle was placed through the crimp cap membrane before the vials were placed in the high-pressure reactor.

Ferredoxin. Aliquots of lyophilized ferredoxin from *C. pasteurianum* prepared in *E. coli* as described (55) were suspended in 3.5 mL of N_2-washed phosphate buffer per reaction with 100 nmol Fd distributed throughout the experimental run (one replica for Ni_xFe and Fe_3O_4 and three replicas for all other reactions) and the control. 0.8 mL of the solution was placed on top of 0.1 mmol iron powder (Fe^0, 99.9+% metals basis, particle size <10 μm, Alfa Aesar), cobalt powder (Co^0, metal basis, particle size 1.6 μm, Alfa Aesar), nickel powder (Ni^0, metal basis, particle size 3 to 7 μm, Alfa Aesar), molybdenum powder (Mo^0, 100 Mesh, 99.95% metal basis, Alfa Aesar), magnetite (Fe_3O_4, 97% trace metal basis, particle size 50 to 100 nm, Sigma-Aldrich), or Ni_xFe (synthesis based on (30), kindly provided by Tuğçe Beyazay, Max Planck Institute for Coal Research, Mülheim, Germany). The remaining volume of the Fd stock was used as a pre-reaction control for UV-Vis spectroscopy. The ferredoxin and hydrogenase structures in Fig. 1 were rendered with Pymol (103).

Reaction. After pressurizing the reactor with either 5 bar of Ar gas (99.998%, Air Liquide) or 5 bar of H_2 gas (99.999%, Air Liquide), reactions were started and regulated by a temperature controller (BTC-3000, Berghof Products + Instruments GmbH). Reactions were performed at 40 °C. The reaction time spanned from 1 h to 4 h. Afterward, reactors were depressurized under anaerobic conditions and the samples (metal powders and solution) were transferred to 2-mL Eppendorf tubes and centrifuged for 15 min at 13,000 rpm (Biofuge Fresco, Hereaeus). Supernatants were analyzed.

Reduction with Sodium Dithionite. To obtain standards of Fd, the protein was reduced using sodium dithionite (ACROS Organics, Geel). Ferredoxin was diluted in a N_2-washed 133 mM phosphate buffer solution (pH 8.5). Sodium dithionite was prepared in a similar solution at pH 8.6. The reduction was carried out with two moles of sodium dithionite per one mole of ferredoxin. In a 3-mL UV quartz cuvette with a small PTFE-coated stirring bar at 400 rpm, reduced Fd was re-oxidized by air, measuring a full scan of the UV-Vis spectrum every 30 s until the protein was re-oxidized.

UV-Vis Spectrophotometry. Spectra were recorded in an Agilent Technologies Cary 300 UV-Vis Compact Peltier spectrophotometer using UV-quartz cuvettes covered with a rubber stopper. A 200 to 800 nm scan was taken for each sample. Absorption of the [4Fe4S] clusters in Fd was normalized to the absorbance of the isosbestic point of the spectrum at 354 nm (56). Data were analyzed with

the Cary UV Workstation and Cary WinUV software. Midpoint potentials of H_2 were calculated with the Nernst equation for the standard hydrogen electrode.

Data, Materials, and Software Availability. PDF data have been deposited in HHU ResearchData (https://doi.org/10.25838/d5p-51) (104).

ACKNOWLEDGMENTS. We thank Dr. Tuğçe Beyazay of the Max Planck Institute for Coal Research, Mülheim, Germany for preparing the Ni_xFe alloys. This project has received funding from the European Research Council (ERC) under the European Union's Horizon 2020 research and innovation programme (grant agreement no. 101018894). For funding, W.F.M. thanks the ERC (101018894), the Deutsche Forschungsgemeinschaft (MA 1426/21-1), and the Volkswagen Foundation (Grant 96_742), H.T. thanks the Max-Planck Gesellschaft, the Deutsche Forschungsgemeinschaft (TU 315/8-1) and the Volkswagen Foundation (96_742), J.S. thanks the Thailand Research Fund (RSA5980062), Z.-I.K. thanks the Japan Society for the Promotion of Science (20KK0343) and National Institute of Technology (KOSEN) for a sabbatical stipend to Düsseldorf, and W.B. and M.P. thank the Max-Planck Gesellschaft.

Author affiliations: [a]Institute of Molecular Evolution, Faculty of Mathematics and Natural Sciences, Heinrich Heine University Düsseldorf, Düsseldorf 40225, Germany; [b]Microcosm Earth Center, Research Group for Geochemical Protozymes, Max Planck Institute for Terrestrial Microbiology and Philipps University, Marburg 35032, Germany; [c]Department of Civil and Environmental Engineering, National Institute of Technology, Kure College, Kure, Hiroshima 737-8506, Japan; [d]Department of Biochemistry, Chulalongkorn University, Patumwan, Bangkok 10330, Thailand; [e]Institute for Physical Chemistry, Faculty of Mathematics and Natural Sciences, Heinrich Heine University Düsseldorf, Düsseldorf 40225, Germany; [f]Max Planck Institute for Coal Research, Department of Heterogeneous Catalysis, Mülheim an der Ruhr 45470, Germany; [g]Max Planck Institute for Terrestrial Microbiology, Marburg 35043, Germany; [h]Laboratory for Microbiology, Department of Biology, Philipps University, Marburg 35043, Germany; and [i]Center for Synthetic Microbiology SYNMIKRO, Philipps University, Marburg 35043, Germany

1. G. Fuchs, E. Stupperich, "Evolution of autotrophic CO_2 fixation" in *Evolution of Prokaryotes*, K. Schleifer, E. Stackenbrandt, Eds. (Academic Press, London, 1985), pp. 235–251.
2. G. Fuchs, Alternative pathways of carbon dioxide fixation: Insights into the early evolution of life? *Annu. Rev. Microbiol.* **65**, 631–658 (2011).
3. I. A. Berg, Ecological aspects of the distribution of different autotrophic CO_2 fixation pathways. *Appl. Environ. Microbiol.* **77**, 1925–1936 (2011).
4. T. Wagner, U. Ermler, S. Shima, The methanogenic CO_2 reducing-and-fixing enzyme is bifunctional and contains 46 [4Fe-4S] clusters. *Science* **354**, 114–117 (2016).
5. M. Can, F. A. Armstrong, S. W. Ragsdale, Structure, function, and mechanism of the nickel metalloenzymes, CO dehydrogenase, and acetyl-CoA synthase. *Chem. Rev.* **114**, 4149–4174 (2014).
6. M. H. Charon, A. Volbeda, E. Chabriere, L. Pieulle, J. C. Fontecilla-Camps, Structure and electron transfer mechanism of pyruvate:ferredoxin oxidoreductase. *Curr. Opin. Struct. Biol.* **9**, 663–669 (1999).
7. H. Dobbek, V. Svetlitchnyi, L. Gremer, R. Huber, O. Meyer, Crystal structure of a carbon monoxide dehydrogenase reveals a [Ni-4Fe-5S] cluster. *Science* **293**, 1281–1285 (2001).
8. S. Shima, G. Huang, T. Wagner, U. Ermler, Structural basis of hydrogenotrophic methanogenesis. *Annu. Rev. Microbiol.* **74**, 713–733 (2020).
9. F. Lipmann, "Projecting backward from the present stage of evolution of biosynthesis" in *The Origin of Prebiological Systems and of their Molecular Matrices*, S. W. Fox, Ed. (Academic Press, New York, NY, 1965), pp. 259–280.
10. R. V. Eck, M. O. Dayhoff, Evolution of the structure of ferredoxin based on living relics of primitive amino acid sequences. *Science* **152**, 363–366 (1966).
11. D. O. Hall, R. Cammack, K. K. Rao, Role for ferredoxins in the origin of life and biological evolution. *Nature* **233**, 136–138 (1971).
12. G. Caserta *et al.*, Unusual structures and unknown roles of FeS clusters in metalloenzymes seen from a resonance Raman spectroscopic perspective. *Coord. Chem. Rev.* **452**, 214287 (2022).
13. J. A. Baross, S. E. Hoffman, Submarine hydrothermal vents and associated gradient environments as sites for the origin and evolution of life. *Orig. Life Evol. Biosph.* **15**, 327–345 (1985).
14. N. Mrnjavac, J. L. E. Wimmer, M. Brabender, L. Schwander, W. F. Martin, The Moon-forming impact and the autotrophic origin of life. *ChemPlusChem.* **88**, e202300270 (2023).
15. N. H. Sleep, D. K. Bird, E. C. Pope, Serpentinite and the dawn of life. *Philos. Trans. R. Soc. Lond. B Biol. Sci.* **366**, 2857–2869 (2011).
16. R. Tamblyn, J. Hermann, Geological evidence for high H_2 production from komatiites in the Archaean. *Nat. Geosci.* **16**, 1194–1199 (2023).
17. M. Preiner *et al.*, A hydrogen-dependent geochemical analogue of primordial carbon and energy metabolism. *Nat. Ecol. Evol.* **4**, 534–542 (2020).
18. K. S. Belthle *et al.*, Effects of silica modification (Mg, Al, Ca, Ti, and Zr) on supported cobalt catalysts for H_2 dependent CO_2 reduction to metabolic intermediates. *J. Am. Chem. Soc.* **144**, 21232–21243 (2022).
19. T. Beyazay *et al.*, Influence of composition of nickel-iron nanoparticles for abiotic CO_2 conversion to early prebiotic organics. *Angew. Chem. Int. Ed. Engl.* **62**, e202218189 (2023).
20. T. Beyazay *et al.*, Ambient temperature CO_2 fixation to pyruvate and subsequently to citramalate over iron and nickel nanoparticles. *Nat. Commun.* **14**, 570 (2023).
21. J. A. Chamberlain, C. R. McLeod, R. J. Traill, G. R. Lachance, Native metals in the Muskox intrusion. *Can. J. Earth Sci.* **2**, 188–215 (1965).
22. C. Kanellopoulos *et al.*, A new occurrence of terrestrial native iron in the Earth's surface: The Ilia thermogenic travertine case, northwestern Euboea, Greece. *Geosciences* **8**, 287 (2018).
23. P. K. Kepezhinskas, N. P. Kepezhinskas, N. V. Berdnikov, V. O. Krutikova, Native metals and intermetallic compounds in subduction-related ultramafic rocks from the Stanovoy mobile belt (Russian Far East): Implications for redox heterogeneity in subduction zones. *Ore Geol. Rev.* **127**, 103800 (2020).
24. C. Furdui, S. W. Ragsdale, The role of pyruvate ferredoxin oxidoreductase in pyruvate synthesis during autotrophic growth by the Wood–Ljungdahl pathway. *J. Biol. Chem.* **275**, 28494–28499 (2000).
25. R. K. Thauer, K. Jungermann, K. Decker, Energy conservation in chemotrophic anaerobic bacteria. *Bacteriol. Rev.* **41**, 100–180 (1977).
26. D. R. Colman *et al.*, Deep-branching acetogens in serpentinized subsurface fluids of Oman. *Proc. Natl. Acad. Sci. U.S.A.* **119**, e2206845119 (2022).
27. M. O. Schrenk, D. S. Kelley, S. A. Bolton, J. A. Baross, Low archaeal diversity linked to subseafloor geochemical processes at the Lost City hydrothermal field, mid-Atlantic ridge. *Environ. Microbiol.* **6**, 1086–1095 (2004).
28. E. M. Fones *et al.*, Diversification of methanogens into hyperalkaline serpentinizing environments through adaptations to minimize oxidant limitation. *ISME J.* **15**, 1121–1135 (2021).
29. S. Q. Lang, W. J. Brazelton, Habitability of the marine serpentinite subsurface: A case study of the Lost City hydrothermal field. *Philos. Trans. A Math. Phys. Eng. Sci.* **378**, 20180429 (2020).
30. S. Suzuki, K. H. Nealson, S. Ishii, Genomic and *in-situ* transcriptomic characterization of the candidate phylum NPL-UPL2 From highly alkaline highly reducing serpentinized groundwater. *Front. Microbiol.* **9**, 3141 (2018).
31. W. Buckel, R. K. Thauer, Energy conservation via electron bifurcating ferredoxin reduction and proton/Na^+ translocating ferredoxin oxidation. *Biochim. Biophys. Acta* **1827**, 94–113 (2013).
32. G. Herrmann, E. Jayamani, G. Mai, W. Buckel, Energy conservation via electron-transferring flavoprotein in anaerobic bacteria. *J. Bacteriol.* **190**, 784–791 (2008).
33. F. Li *et al.*, Coupled ferredoxin and crotonyl coenzyme A (CoA) reduction with NADH catalyzed by the butyryl-CoA dehydrogenase/Etf complex from *Clostridium kluyveri*. *J. Bacteriol.* **190**, 843–850 (2008).
34. A. K. Kaster, J. Moll, K. Parey, R. K. Thauer, Coupling of ferredoxin and heterodisulfide reduction via electron bifurcation in hydrogenotrophic methanogenic archaea. *Proc. Natl. Acad. Sci. U.S.A.* **108**, 2981–2986 (2011).
35. V. Müller, N. P. Chowdhury, M. Basen, Electron bifurcation: A long-hidden energy-coupling mechanism. *Annu. Rev. Microbiol.* **72**, 331–353 (2018).
36. T. Wagner, J. Koch, U. Ermler, S. Shima, Methanogenic heterodisulfide reductase (HdrABC-MvhAGD) uses two noncubane [4Fe-4S] clusters for reduction. *Science* **357**, 699–703 (2017).
37. A. Katsyv *et al.*, Molecular basis of the electron bifurcation mechanism in the [FeFe]-hydrogenase complex HydABC. *J. Am. Chem. Soc.* **145**, 5696–5709 (2023).
38. C. E. Lubner *et al.*, Mechanistic insights into energy conservation by flavin-based electron bifurcation. *Nat. Chem. Biol.* **13**, 655–659 (2017).
39. W. Buckel, R. K. Thauer, Flavin-based electron bifurcation, a new mechanism of biological energy coupling. *Chem. Rev.* **118**, 3862–3886 (2018).
40. G. J. Schut *et al.*, An abundant and diverse new family of electron bifurcating enzymes with a non-canonical catalytic mechanism. *Front. Microbiol.* **13**, 946711 (2022).
41. K. Kayastha, S. Vitt, W. Buckel, U. Ermler, Flavins in the electron bifurcation process. *Arch. Biochem. Biophys.* **701**, 108796 (2021).
42. J. W. Peters, A. F. Miller, A. K. Jones, P. W. King, M. W. Adams, Electron bifurcation. *Curr. Opin. Chem. Biol.* **31**, 146–152 (2016).
43. R. K. Thauer, A.-K. Kaster, H. Seedorf, W. Buckel, R. Hedderich, Methanogenic archaea: Ecologically relevant differences in energy conservation. *Nat. Rev. Microbiol.* **6**, 579–591 (2008).
44. K. Schuchmann, V. Müller, Autotrophy at the thermodynamic limit of life: A model for energy conservation in acetogenic bacteria. *Nat. Rev. Microbiol.* **12**, 809–821 (2014).
45. W. F. Martin, Hydrogen, metals, bifurcating electrons, and proton gradients: The early evolution of biological energy conservation. *FEBS Lett.* **586**, 485–493 (2012).
46. E. S. Boyd, M. J. Amenabar, S. Poudel, A. S. Templeton, Bioenergetic constraints on the origin of autotrophic metabolism. *Philos. Trans. A Math. Phys. Eng. Sci.* **378**, 20190151 (2020).
47. E. M. Shepard *et al.*, [FeFe]-Hydrogenase maturation. *Biochemistry* **53**, 4090–4104 (2014).
48. J. W. Peters *et al.*, [FeFe]- and [NiFe]-hydrogenase diversity, mechanism, and maturation. *Biochim. Biophys. Acta Mol. Cell Res.* **1853**, 1350–1369 (2015).
49. R. D. Britt, G. Rao, L. Tao, Bioassembly of complex iron–sulfur enzymes: Hydrogenases and nitrogenases. *Nat. Rev. Chem.* **4**, 542–549 (2020).
50. D. W. Mulder *et al.*, Stepwise [FeFe]-hydrogenase H-cluster assembly revealed in the structure of $HydA^{\Delta EFG}$. *Nature* **465**, 248–252 (2010).
51. S. J. Mojzsis *et al.*, Evidence for life on Earth before 3, 800 million years ago. *Nature* **384**, 55–59 (1996).
52. Y. Ueno, K. Yamada, N. Yoshida, S. Maruyama, Y. Isozaki, Evidence from fluid inclusions for microbial methanogenesis in the early archaean era. *Nature* **440**, 516–519 (2006).
53. H. Takami *et al.*, A deeply branching thermophilic bacterium with an ancient acetyl-CoA pathway dominates a subsurface ecosystem. *PLoS One* **7**, e30559 (2012).
54. D. S. Kelley *et al.*, A serpentinite-hosted ecosystem: The Lost City hydrothermal field. *Science* **307**, 1428–1434 (2005).
55. L. Schwander *et al.*, Serpentinization as the source of energy, electrons, organics, catalysts, nutrients and pH gradients for the origin of LUCA and life. *Front. Microbiol.* **14**, 1257597 (2023).
56. J. Sucharitakul *et al.*, Modulations of the reduction potentials of flavin-based electron bifurcation complexes and semiquinone stabilities are key to control directional electron flow. *FEBS J.* **288**, 1008–1026 (2021).
57. D. P. Henriques Pereira *et al.*, Role of geochemical protoenzymes (geozymes) in primordial metabolism: Specific abiotic hydride transfer by metals to the biological redox cofactor NAD^+. *FEBS J.* **289**, 3148–3162 (2022).
58. R. C. Prince, M. W. Adams, Oxidation-reduction properties of the two Fe_4S_4 clusters in *Clostridium pasteurianum* ferredoxin. *J. Biol. Chem.* **262**, 5125–5128 (1987).

59. W. Thamer *et al.*, A two [4Fe-4S]-cluster-containing ferredoxin as an alternative electron donor for 2-hydroxyglutaryl-CoA dehydratase from *Acidaminococcus fermentans*. *Arch. Microbiol.* **179**, 197–204 (2003).
60. S. Menon, S. W. Ragsdale, Unleashing hydrogenase activity in carbon monoxide dehydrogenase/acetyl-CoA synthase and pyruvate:ferredoxin oxidoreductase. *Biochemistry* **35**, 15814–15821 (1996).
61. K. Christmann, Interaction of hydrogen with solid surfaces. *Surf. Sci. Rep.* **9**, 1–163 (1988).
62. D. R. Aireddy, K. Ding, Heterolytic dissociation of H_2 in heterogeneous catalysis. *ACS Catal.* **12**, 4707–4723 (2022).
63. R. S. Magliozzo, B. A. McIntosh, W. V. Sweeney, Origin of the pH dependence of the midpoint reduction potential in *Clostridium pasteurianum* ferredoxin: Oxidation state-dependent hydrogen ion association. *J. Biol. Chem.* **257**, 3506–3509 (1982).
64. S. Kato, I. Yumoto, Y. Kamagata, Isolation of acetogenic bacteria that induce biocorrosion by utilizing metallic iron as the sole electron donor. *Appl. Environ. Microbiol.* **81**, 67–73 (2015).
65. J. Philips, Extracellular electron uptake by acetogenic bacteria: Does H_2 consumption favor the H_2 evolution reaction on a cathode or metallic iron? *Front. Microbiol.* **10**, 2997 (2020).
66. D. Xu, T. Gu, D. R. Lovley, Microbially mediated metal corrosion. *Nat. Rev. Microbiol.* **21**, 705–718 (2023).
67. A. J. Bard, R. Parsons, J. Jordan, *Standard Potentials in Aqueous Solution* (CRC Press, Boca Raton, 1985).
68. C. C. Page, C. C. Moser, X. Chen, P. L. Dutton, Natural engineering principles of electron tunnelling in biological oxidation–reduction. *Nature* **402**, 47–52 (1999).
69. H. B. Gray, J. R. Winkler, Electron tunneling through proteins. *Q. Rev. Biophys.* **36**, 341–372 (2003).
70. A. Roldan *et al.*, Bio-inspired CO_2 conversion by iron sulfide catalysts under sustainable conditions. *Chem. Commun.* **51**, 7501–7504 (2015).
71. N. Kitadai *et al.*, Thioester synthesis through geoelectrochemical CO_2 fixation on Ni sulfides. *Commun. Chem.* **4**, 37 (2021).
72. M. C. Weiss *et al.*, The physiology and habitat of the last universal common ancestor. *Nat. Microbiol.* **1**, 1–8 (2016).
73. T. A. Williams *et al.*, Integrative modeling of gene and genome evolution roots the archaeal tree of life. *Proc. Natl. Acad. Sci. U.S.A.* **114**, E4602–E4611 (2017).
74. R. Mei, M. Kaneko, H. Imachi, M. K. Nobu, The origin and evolution of methanogenesis and *Archaea* are intertwined. *PNAS Nexus* **31**, pgad023 (2023).
75. R. Hedderich, Energy-converting (NiFe) hydrogenases from archaea and extremophiles: Ancestors of complex I. *J. Bioenerg. Biomembr.* **36**, 65–75 (2004).
76. M. C. Schoelmerich, V. Müller, Energy conservation by a hydrogenase-dependent chemiosmotic mechanism in an ancient metabolic pathway. *Proc. Natl. Acad. Sci. U.S.A.* **116**, 6329–6334 (2019).
77. N. Lane, W. F. Martin, The origin of membrane bioenergetics. *Cell* **151**, 1406–1416 (2012).
78. S. A. Harrison *et al.*, Life as a guide to its own origins. *Annu. Rev. Ecol. Evol. Syst.* **54**, 327–350 (2023).
79. E. S. Boyd, G. J. Schut, M. W. W. Adams, J. W. Peters, Hydrogen metabolism and the evolution of biological respiration. *Microbe* **9**, 361–367 (2014).
80. K. B. Muchowska, S. J. Varma, J. Moran, Nonenzymatic metabolic reactions and life's origins. *Chem. Rev.* **120**, 7708–7744 (2020).
81. S. J. Varma, K. B. Muchowska, P. Chatelain, J. Moran, Native iron reduces CO_2 to intermediates and end-products of the acetyl-CoA pathway. *Nat. Ecol. Evol.* **2**, 1019–1024 (2018).
82. F. L. Sousa, M. Preiner, W. F. Martin, Native metals, electron bifurcation, and CO_2 reduction in early biochemical evolution. *Curr. Opin. Microbiol.* **43**, 77–83 (2018).
83. T. M. McCollom, J. S. Seewald, Serpentinites, hydrogen, and life. *Elements* **9**, 129–134 (2013).
84. W. Martin, M. J. Russell, On the origin of biochemistry at an alkaline hydrothermal vent. *Philos. Trans. R. Soc. Lond. B Biol. Sci.* **362**, 1887–1926 (2007).
85. C. Schöne *et al.*, Deconstructing *Methanosarcina acetivorans* into an acetogenic archaeon. *Proc. Natl. Acad. Sci. U.S.A.* **119**, e2113853119 (2022).
86. D. D. Sasselov, J. P. Grotzinger, J. D. Sutherland, The origin of life as a planetary phenomenon. *Sci. Adv.* **6**, eaax3419 (2020).
87. S. A. Benner *et al.*, When did life likely emerge on earth in an RNA-first process? *ChemSystemsChem* **2**, e1900035 (2020).
88. B. Damer, D. Deamer, The hot spring hypothesis for an origin of life. *Astrobiology* **20**, 429–452 (2020).
89. B. H. Patel, C. Percivalle, D. J. Ritson, C. D. Duffy, J. D. Sutherland, Common origins of RNA, protein and lipid precursors in a cyanosulfidic protometabolism. *Nat. Chem.* **7**, 301–307 (2015).
90. P. Canavelli, S. Islam, M. W. Powner, Peptide ligation by chemoselective aminonitrile coupling in water. *Nature* **571**, 546–549 (2019).
91. S. Becker *et al.*, Unified prebiotically plausible synthesis of pyrimidine and purine RNA ribonucleotides. *Science* **366**, 76–82 (2019).
92. R. E. Eakin, An approach to the evolution of metabolism. *Proc. Natl. Acad. Sci. U.S.A.* **49**, 360–366 (1963).
93. W. F. Martin, Older than genes: The acetyl CoA pathway and origins. *Front. Microbiol.* **11**, 817 (2020).
94. K. B. Muchowska, S. J. Varma, J. Moran, Synthesis and breakdown of universal metabolic precursors promoted by iron. *Nature* **569**, 104–107 (2019).
95. J. L. E. Wimmer *et al.*, Energy at origins: Favorable thermodynamics of biosynthetic reactions in the last universal common ancestor (LUCA). *Front. Microbiol.* **12**, 793664 (2021).
96. R. J. Mayer, J. Moran, Quantifying reductive amination in nonenzymatic amino acid synthesis. *Angew. Chem. Int. Ed. Engl.* **61**, e202212237 (2022).
97. J. Yi *et al.*, A nonenzymatic analog of pyrimidine nucleobase biosynthesis. *Angew. Chem. Int. Ed. Engl.* **61**, e202117211 (2022).
98. W. Nitschke, M. J. Russell, Beating the acetyl coenzyme A-pathway to the origin of life. *Philos. Trans. R. Soc. Lond. B Biol. Sci.* **368**, 20120258 (2013).
99. O. Farr *et al.*, Methanol on the rocks: Green rust transformation promotes the oxidation of methane. *J. Roy. Soc. Interface* **20**, 20230386 (2023).
100. G. Wächtershäuser, Before enzymes and templates: Theory of surface metabolism. *Microbiol. Rev.* **52**, 452–484 (1988).
101. E. Smith, H. J. Morowitz, *The Origin and Nature of Life on Earth* (Cambridge University Press, 2016).
102. Z. Mao *et al.*, AMP-dependent phosphite dehydrogenase, a phosphorylating enzyme in dissimilatory phosphite oxidation. *Proc. Natl. Acad. Sc.i U.S.A.* **120**, e230974312 (2023).
103. L. L. C. Schrödinger, The PyMOL Molecular Graphics System (Version 2.5.4, 2022). https://pymol.org/2/. Accessed 23 October 2023.
104. M. Brabender *et al.*, Ferredoxin reduction by hydrogen with iron functions as an evolutionary precursor of flavin-based electron bifurcation. HHU ResearchData. https://doi.org/10.25838/d5p-51. Deposited 3 November 2023.